THE EFFECT OF THE MICROSTRUCTURE ON THE TRIBOLOGICAL PROPERTIES OF THE MONEL K-500 ALLOY

KRAWCZYK Janusz, FROCISZ Łukasz, MATUSIEWICZ Piotr, MADEJ Marcin

AGH University of Science and Technology, Faculty of Metals Engineering and Industrial Computer Science, Cracow, Poland, EU, jkrawcz@agh.edu.pl

Abstract

The aim of the work was to determine the microstructure effect on the tribological properties of the Monel K-500 alloy. The supersaturation temperature of 1150 °C was selected in such a way so that it would exceed the solution temperature of the carbides present in the Monel K-500 alloy by less than 10 °C. For the annealing temperature assumed in this way, the annealing time was assumed to be 1 h, 2 h and 4 h. Ageing at the temperature of 595 °C for 8 h was also performed, followed by cooling at the rate of 0.2 °C / min down to the temperature of 480 °C. Further cooling was continued in air. The evaluation of the test results was based on hardness measurements, a friction test as well as a stereological evaluation of the grain. It was stated that the hardness is not a factor which determines the tribological wear resistance of the Monel K-500 alloy. The deciding factor for the tribological wear resistance is the dominant wear mechanisms. The Monel K-500 alloy exhibits a higher wear resistance in the supersaturated state than the aged state after supersaturation. The grain growth seems to result in a reduction of wear and an increase of the friction coefficient in the case of samples aged after supersaturation.

Keywords: Nickel alloy, Monel K-500, wear, microstructure, grain size

1.   INTRODUCTION

The lack of allotropic forms of nickel causes limitations in the formation of the microstructure of its alloys [1]. In this case, the possibilities of controlling the grain size by way of thermal treatment are limited [2, 3]. However, to that end, we can use plastic working with the application of recrystallization (often dynamic recrystallization) [4-6]). The proceeding development of nickel alloys as well as the examinations that follow, characterizing these materials, consider the tribological properties as one of the crucial parameters for the designing of these materials [7-10]. Also in the case of the already well-known nickel alloys, such as Monel K-500 [11-14], we can observe interest in their tribological properties [15-17]. Unfortunately, these works refer to the microstructure of this alloy and its role in the tribological properties only to a little extent. Due to this fact, the aim of this work was to determine the effect of the microstructure on the tribological properties of the Monel K-500 alloy.

2.   MATERIAL FOR INVESTIGATION

The chemical composition of the examined alloy is included in **Table 1**. The material is characterized in grain heterogeneity (**Fig. 1**). On the basis of the Feret's diameter determined in different areas and sections of the bar (material in the form as-delivered), we can state no significant differences in the microstructure of the section of the bar (**Table 2**). However, in the analysis of the mean surface area of the section, a finer grain was observed at the surface of the bar as compared to the bar's axis (**Table 2**). What is more, by analyzing such parameters as the standard error, the range, the maximal value and the standard deviation, we can observe a more sigificant heterogeneity of the grain in the bar's axis than in its edge (**Table 3**). The analysis of the kurtosis suggests that the distribution of the grain size is much more slender than in the case of the normal distribution, which proves a specific concentration of the grain size for its strictly defined values. In the analyzed microstructure, this should be referred to the areas of a fine grain. By understanding the kurtosis values in this way, we can state that the fine grain areas in the axis of the bar characterize in its high heterogeneity. Probably, the grain size difference in the initial material resulted from a lower stage of

advancement of the recrystallization process (dynamic recrystallization) in the axis of the bar. The grain formed as a result of the recrystllization process in the bar's axis did not grow in the direction of the non-recrystallized grains to such a degree as in the vicinity of the bar's edge. In analyzing the parameter described as skewness, we can observe more larger than smaller grains in reference to the mean value (positive skewness). This paramer also points to a lower stage of advancement of the resrystallization process in the axis of the bar as compared to its edge (**Table 2**). And so, the hardness of the material depends on the area of the measurement and equals 150 HV in the bar's axis and 193 HV in the vicinity of its edge.

Table 1 Chemical composition (wt. %) of the Monel K-500 alloy

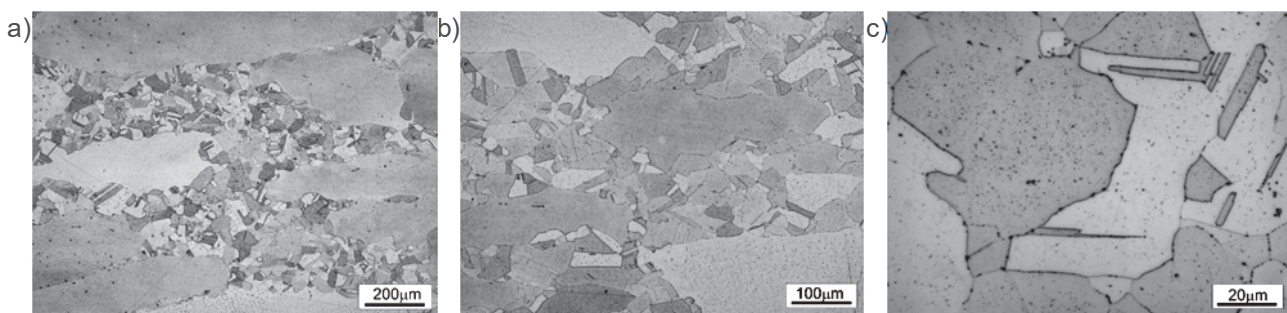| C	Cu	Al	Fe	Mn	Ti	Si	Co	S	Ni
0.12	30.15	3.02	1.01	0.62	0.60	0.15	0.001	0.001	Bal.

Fig. 1 Microstructure of the Monel K-500 alloy as delivered conditions

Table 2 Description parameters characterizing the results of the grain morphology measurements in the material as-delivered depending on the microstructure area

parameters	as delivered conditions		
	longitudinal section	cross-section, edge of the bar	cross-section, core of the bar
Feret diameter			
average (µm)	8.7	8.9	8.2
standard error of the mean (µm)	0.4	0.5	0.2
mode (µm)	4.1	2.4	7.4
the maximum value (µm)	86	121	66
standard deviation (µm)	8.1	10.1	5.8
kurtosis	30.6	58.5	32.1
bias	4.7	6.5	4.3
sample size	523	449	749
cross-sectional area of grain			
average (µm^2)	110	142	79
standard error of the mean (µm^2)	17	35	8
mode (µm^2)	45	4	43
the maximum value (µm^2)	5882	11489	3459
standard deviation (µm^2)	387	741	213
kurtosis	113.2	166.9	154.3
bias	9.5	12.3	11.4
sample size	523	449	749

It is known that there is a possibility to unify the grain size through its growth as a result of the material's annealing at the appropriately high temperature and for a proper period of time [18]. And so, the examined material was annealed and supersaturated, which aimed at homogenization of the grain size (**Fig. 2**). The samples were annealed at 1150 °C for 1 h (hour), 2 h and 4 h and next supersaturated in water. The supersaturation temperature, 1150 °C, was selected in such a way so as to exceed the temperature of dissolution of the carbides present in the Monel K-500 alloy by less than 10 °C. Aging of the supersaturated material at 595 °C for 8 h was also performed, followed by cooling at the rate of 0.2 °C / min (12 K / h) down to 480 °C and further cooling in air. As a result of the annealing and supersaturation, homogenization of the grain was obtained (**Table 3**). A compilation of the hardness measurement results for the material in the state after supersaturation and ageing, for different times of annealing until supersaturation was achieved, is included in **Table 4**.

Table 3 The results of measurements of grain morphology of the material in a supersaturated state

| parameters	Feret diameter			cross-sectional area of grain		
	1 h	2 h	4 h	1 h	2 h	4 h
average	31.4 μm	33.9 μm	34.6 μm	995 μm^2	1222 μm^2	1247 μm^2
standard error of the mean	0.7 μm	0.9 μm	0.9 μm	53 μm^2	78 μm^2	71 μm^2
mode	26.0 μm	25.5 μm	43.5 μm	766 μm^2	622 μm^2	510 μm^2
the maximum value	140 μm	141 μm	133 μm	15343 μm^2	15562 μm^2	13888 μm^2
standard deviation	16.7 μm	20.3 μm	19.7 μm	1256 μm^2	1745 μm^2	1573 μm^2
kurtosis	5.2	4.6	2.7	40.8	24.8	16.3
bias	1.5	1.7	1.4	5.0	4.2	3.4
sample size	560	497	487	560	497	487
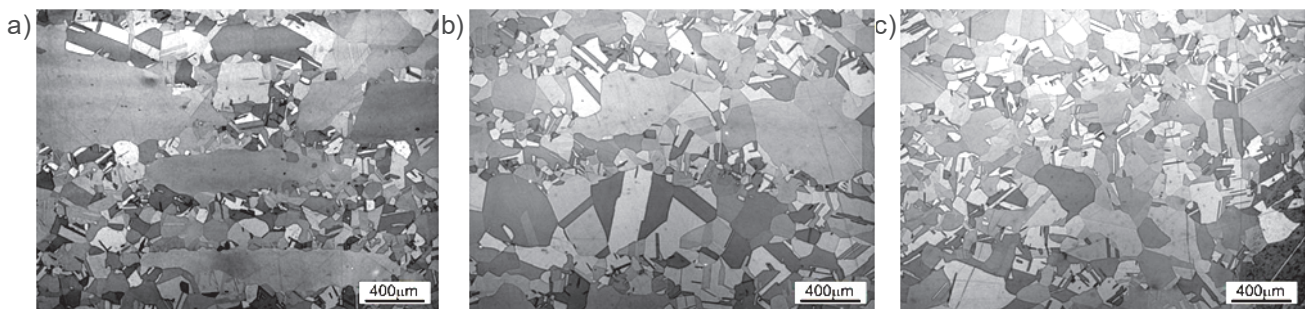
Fig. 2 The microstructure after supersaturation from temperature 1150 °C for the annealing time:
a) 1 h, b) 2 h, c) 4 h

Table 4 Compilation of hardness measurement results for the material after supersaturation, and after supersaturation and ageing, for different annealing times

	supersaturation			aging after supersaturation		
annealing time	1 h	2 h	4 h	1 h	2 h	4 h
average [HV10]	117.2	113.8	113.7	272.3	273.2	274.0
standard error of the mean [HV10]	1.9	2.3	1.1	1.7	3.5	1.8

3. METHODOLOGY OF TRIBOLOGICAL RESEARCH

The tribological tests were performed by means of the T-05 tester with the block on roll friction couple, at room temperature. The measurements were performed on the material after annealing as well as after annealing

and supersaturation. The pressure force of the couple on the sample equaled 100 N and the duration time of the tests was 2000 s. The samples for the tribological tests were 4x4x20 mm cuboids. The counter-sample was made of 100Cr6 steel, with the hardness of about 62 HRC (760 HV).

4. RESULTS AND DISCUSSION

Images of the surfaces of the samples supersaturated after the tribological tests are shown in **Fig. 3.** We can observe the occurrence of effects corresponding to adhesive wear. Especially visible are areas characteristic for adhesive wear in the case of the sample annealed until supersaturated for 4 h. Next to adhesive wear, we can also observe effects connected with abrasive wear as well as areas where fragments of the material were ripped off. Also observed are fine particles, which are driven inside the surface, and in some areas, we can see traces of these particles' movement by way of ridging.

The surface of the examined samples, annealed and aged, which underwent tribological wear is presented in **Fig. 4**. We can observe that the samples which aged after supersaturation wear by way of two mechanisms. One is abrasive wear, consisting in micro-machining. The other is chipping as a result of the material's decohesion, probably mainly along the grain boundaries. The intensity of the chipping seems to increase together with the shortening of the time of the samples' ageing up to supersaturation (reduction of grain size). However, the size of the areas of single chippings seems to increase together with the elongation of the time of ageing to supersaturation. This is, however, connected with the increase of the size of the areas exhibiting abrasive wear.
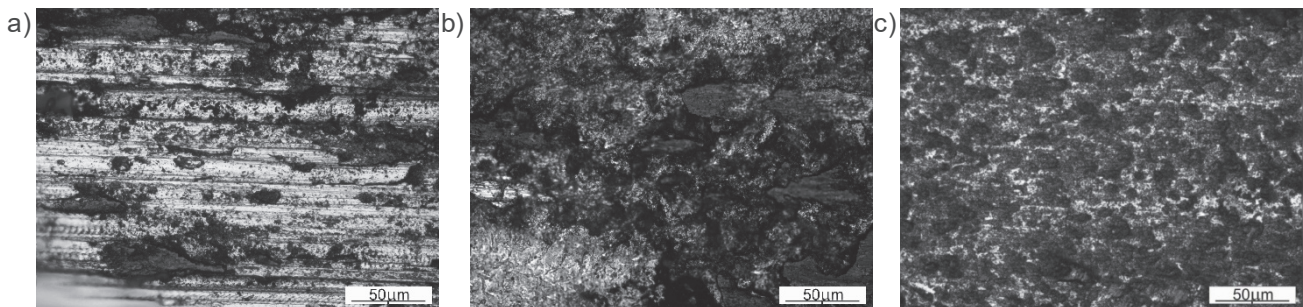

Fig. 3 Tribological contact surfaces on supersaturated samples, annealed to the supersaturation by: a) 1 h, b) 2 h, c) 4 h
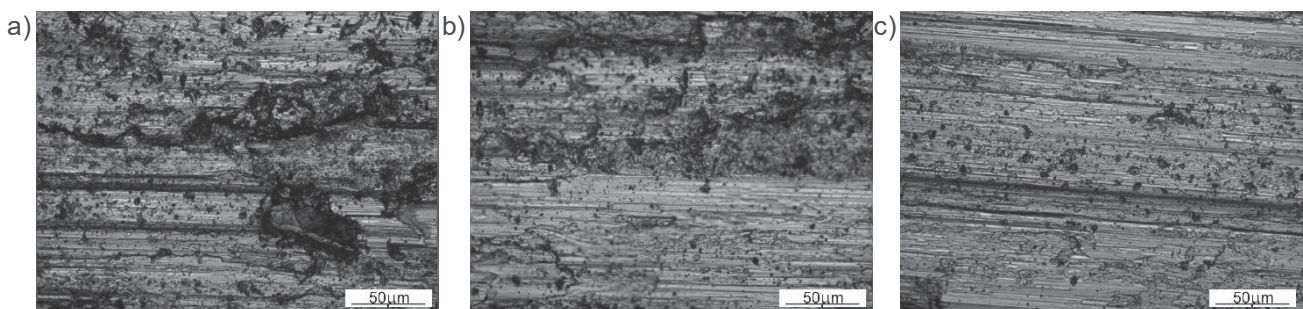

Fig. 4 Tribological contact surfaces on the aged samples after supersaturation, annealed to saturation by: a) 1 h, b) 2 h, c) 4 h

As a result of the tribological tests, it was possible to determine the extent of the wear as well as the mean friction coefficient for the samples which had been only supersaturated as well as those supersaturated and aged (**Fig. 5**). We can observe that the wear of the samples which underwent ageing after supersaturation is much more extensive than in the case of the samples which were only supersaturated. This is interesting in so far as the hardness of the samples after ageing is much higher than that of the samples which have been

only supersaturated (as can be seen in **Table 4**). And so, we can suppose that the factor determining the wear under the applied tribological conditions is the wear mechanism and not the material's hardness. Also visible is an evident effect of the time of annealing to supersaturation in the case of the samples aged after supersaturation. The intensification of the wear together with the shortening of the annealing time up to the samples' supersaturation can result from a finer grain in the case of a shorter time of annealing to supersaturation (**Table 3**). In light of the fact that the materials' decohesion after ageing proceeds especially easily along the grain boundaries (areas of privileged nucleation during ageing), we can observe that the dependence of the wear on the parameters of the thermal treatment seems quite logical. The question arises as to why the supersaturated samples characterize in a much lesser wear than those which have been aged and supersaturated or why there seems to be no dependence of the extent of the wear on the grain size related to the time of annealing to supersaturation. The answer may be connected with the lack of facilitation of the decohesion on the grain boundaries in the case of the samples only supersaturated (**Fig. 5**). The intensification of the adhesive wear can be related to the lack of precipitations (homogeneity) of the material which underwent tribological wear. We should, however, note that on the surface of the only-supersaturated samples, fine particles were observed, which seemed to characterize in a higher hardness as they went deep into the surface of the sample. And so, we can suppose that adhesive wear favours the ripping off of the counter-sample (particles of carbides being part the microstructure of steel 100Cr6), which, in consequence, modifies the properties of the surface layer during the tribological contact. Such a modification of the surface layer can be a factor which strongly hinders a further wear of the material, and the above mentioned samples limit the mass loss of the analyzed samples. We can also observe that, in the case of the sample annealed for 4 h, before supersaturation, the adhesive wear is the highest, which is reflected by a slight increase of the wear of this sample as compared to the one which was annealed for 2 h before supersaturation.

We can observe that the lowest friction coefficient, both in the case of the only-supersaturated samples and those which were supersaturated and aged, was exhibited by those annealed for 1 h before supersaturation. The highest friction coefficient, in turn, was exhibited by the samples annealed for 2 h before supersaturation (**Fig. 5b**). The lowest friction coefficient in the case of the sample of the finest grain (the shortest time of annealing before supersaturation) can be caused by two things. One is the smallest chipped off areas in the case of the samples after such time of annealing which caused their ageing after supersaturation. These chippings are the smallest in size as compared to other aged samples; however, their number significantly limits the friction force connected with the classic abrasive wear, due to the limitation of the areas of such wear. And so, an increase of the grain size by way of increasing the annealing time to 2 h results, in the case of the samples aged after supersaturation, in an increase of the chipped areas and an increase of the machining path. A further increase of the grain size causes a further limitation of the size of the chippings in the case of the aged samples. This lowers the friction force as a result of the increase of the contribution of a third body (chippings) in the process of tribological contact.
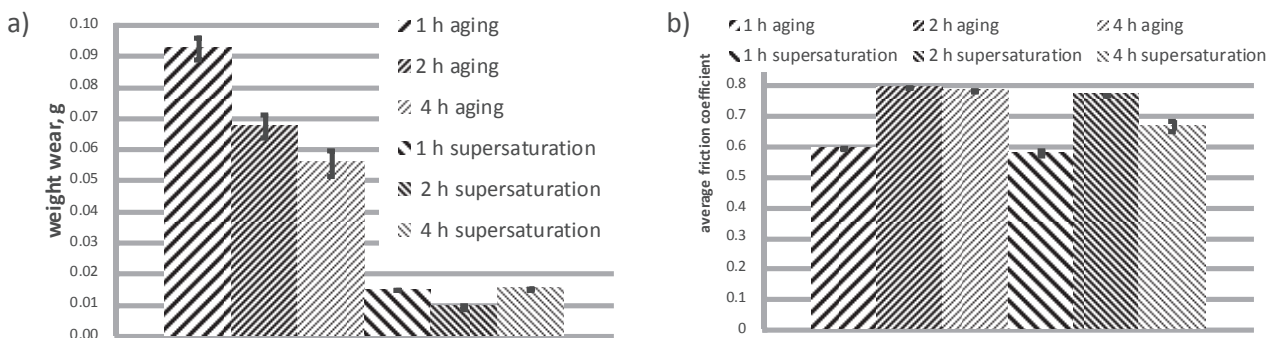

Fig. 5 Tribological parameters of the tested samples: a) the weight wear, b) average friction coefficient

With the aim to assess the relation between the friction coefficient and the mass wear, a diagram included in **Fig. 6** was drawn. We can observe that, especially in the case of the samples aged after supersaturation, an increase of the mean friction coefficient corresponds to a lesser wear of the material. This can result from the modification of the surface layer during the tribological contact in the direction of hardening as well as the increase of the fraction of the hardened particles. This refers to the mechanisms of abrasive wear.
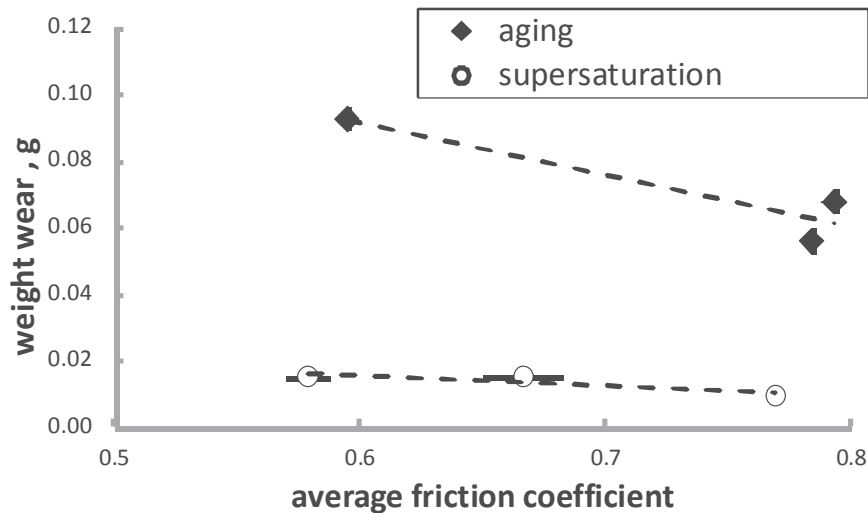

Fig. 6 The relationship between the average friction coefficient and weight wear of test samples

The change in the material's hardness after thermal treatment seems to have no evident effect on the friction coefficient (**Fig. 7a**). However, as it was suggested earlier, a clear influence on the extent of the weight wear of the examined materials is connected with the change of hardness as a result of ageing, which is confirmed by the diagram included in **Fig. 7b**. Additionally, we can point to a possible effect of the slight changes in hardness (within the measurement error) on the wear of the samples aged after supersaturation. And so, we can safely state that an increase of hardness as a result of aging causes a change in the wear mechanism, which intensifies the tribological wear. These points to the fact that we should not always expect an increase of the tribological wear resistance together with the increase of hardness. In this aspect, the mechanism of the tribological contact and the structural characteristics of the material are significant. As it was mentioned earlier, we can observe the expected relation between the reduction of the weight wear and the increase of hardness only in the case of the occurrence of a similar mechanism of tribological wear (with a large contribution of abrasive wear in the case of the samples aged after supersaturation).
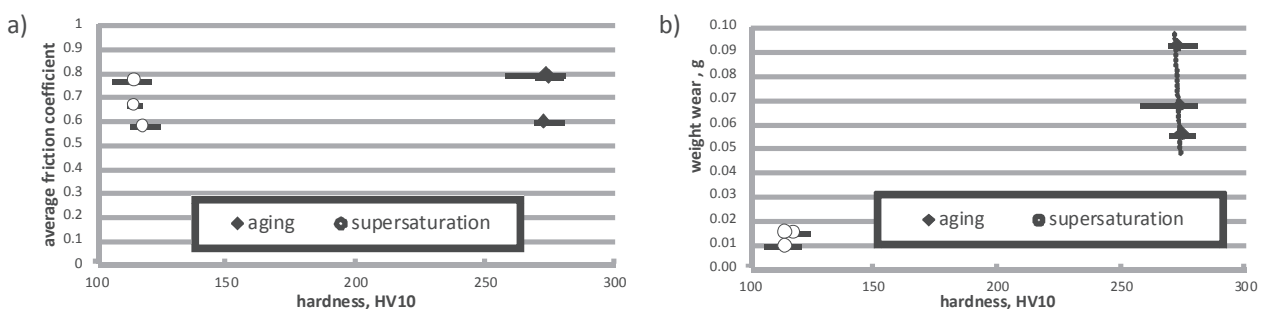

Fig. 7 Effect of hardness at: a) the average friction coefficient, b) weight wear

Another analyzed parameter was the size of the grain. An assessment of the effect of the grain size on the friction coefficient, calculated by the Feret's method and estimated as the mean surface area of the section of the grain, is graphically presented in **Fig. 8**. We can observe a slight tendency of the friction coefficient to grow

together with the increase of the grain size, both in the case of the only-supersaturated samples and those which were aged after supersaturation.
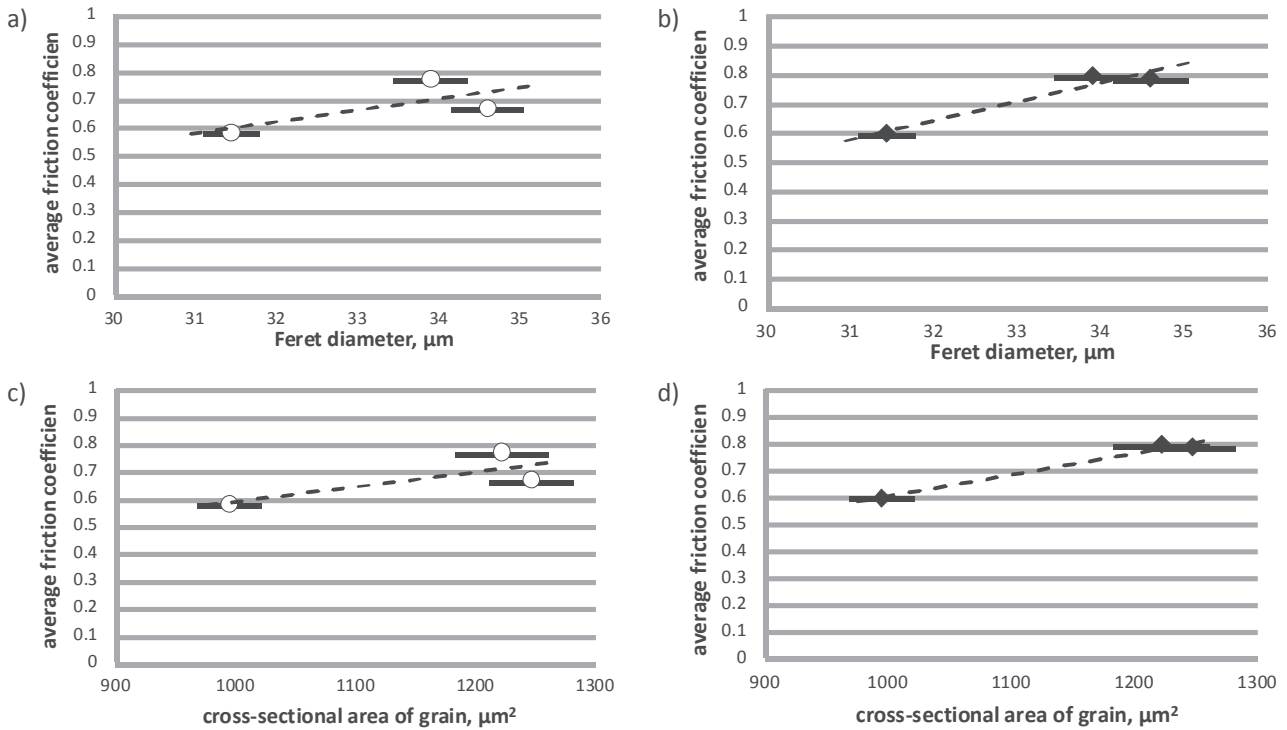

Fig. 8 Effect of the grain size on the mean friction coefficient: a, c) a supersaturated condition, b, d) after aging, a, b) the grain size determined by Feret diameter, c, d) the average cross sectional area of the grain

Fig. 9 The influence of grain size on the wear: a, c) a supersaturated condition, b, d) after aging, a, b) the grain size determined by Feret diameter, c, d) the average cross sectional area of the grain
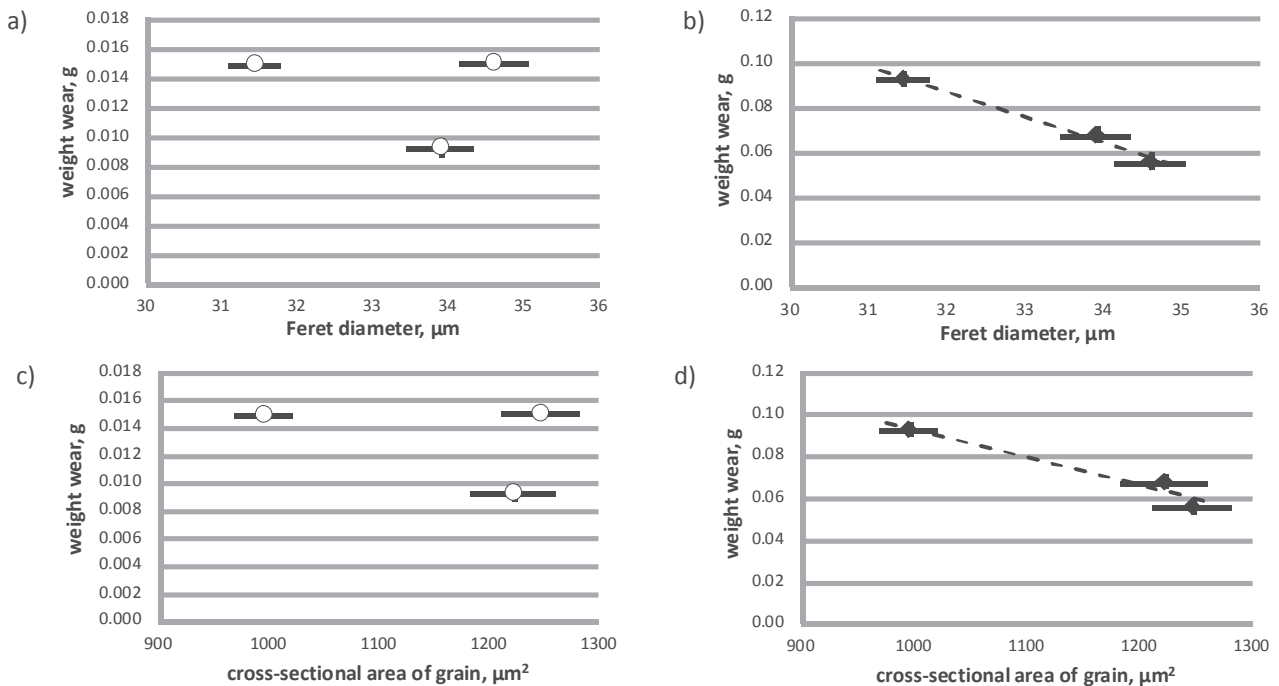
The effect of the grain size on the extent of the wear is presented in **Fig. 9**. As we can see, no clear dependence was obtained in the case of the only-supersaturated samples, whereas, in the case of the samples aged after supersaturation, we can clearly see that together with the increase of the grain size, the extent of the wear decreases. This can be connected with the limitation of the chippings related to decohesion along the grain boundaries in the samples after ageing.

5.   CONCLUSION

The results obtained in this work make it possible to draw the following conclusions as well as make the following observations:

1)   Hardness is not a factor which determines the tribological wear resistance of the Monel K-500 alloy.
2)   A determining factor concerning the tribological wear resistance is the dominant wear mechanisms.
3)   The wear mechanism is dependent on the structural factors of the material undergoing the tribological test.
4)   The Monel K-500 alloy exhibits a higher wear resistance in the supersaturated state than after ageing following the supersaturation.
5)   The precipitation of particles as a result of ageing causes an increase of hardness and a facilitation of decohesion along the grain boundaries as well as limits the adhesive joint during the tribological contact.
6)   In the case of the samples which were only supersaturated, the analysis of the changes in the friction coefficient points to a change in the wear mechanism occurring during the tribological test.
7)   There are premises pointing to a modification of the surface area during the tribological test performed on the samples which were only supersaturated.
8)   The increase of the grain size seems to result in a limitation of the wear as well as an increase of the friction coefficient in the case of the samples aged after supersaturation.

REFERENCES

[1]   DAVIS J.R. (ed.) ASM Specialty handbook - nickel, cobalt and their alloys. ASM International 2000.

[2]   LI Z., ZHANG L., SUN N., FU L., SHAN A. Grain size dependence of the serrated flow in a nickel based alloy. Materials Letters, Vol. 150, 2015, pp. 108-110.

[3]   PARK N.K., PARKER B.A. Effect of grain size on the deformation behavior of nickel and nickel alloy sheet. In Proceedings of the 7th International Conference on the Strength of Metals and Alloys, Montreal, Canada, 12-16 August 1985, pp. 159-164.

[4]   ŁUKASZEK-SOŁEK A., KRAWCZYK J., CHYŁA, P. The analysis of the material flow kinetics during Ni-Fe-Mo alloy forging. Journal of Alloys and Compounds, Vol. 615, 2014, pp. 542-545.

[5]   KRAWCZYK J., ŁUKASZEK-SOŁEK A., ŚLEBODA T., BAŁA P., BEDNAREK S., WOJTASZEK M. Strain induced recrystallization in hot forged Inconel 718 alloy. Archives of Metallurgy and Materials, Vol. 57, 2012,pp. 593-603.

[6]   ŁUKASZEK-SOŁEK A., KRAWCZYK J., BAŁA P., WOJTASZEK M. The analysis of forging Inconel 718 alloy. In METAL 2013: 22nd International Conference on Metallurgy and Materials, Brno, Czech Republic, 2013, pp. 1510-1515.

[7]   BAŁA P. The dilatometric analysis of the high carbon alloys from Ni−Ta−Al−M system. Archives of Metallurgy and Materials, Vol. 59, 2014, pp. 977-980.

[8]   BAŁA P. Microstructure characterization of high carbon alloy from the Ni-Ta-Al-Co-Cr system. Archives of Metallurgy and Materials, Vol. 57, 2012, pp. 937-941.

[9]   BAŁA P. Microstructural characterization of the new tool Ni-based alloy with high carbon and chromium content. Archives of Metallurgy and Materials, Vol. 55, 2010, pp. 1053-1059.

[10]   CIOS G., BAŁA P., STĘPIEŃ M., GÓRECKI K. Microstructure of cast Ni-Cr-Al-C alloy. Archives of Metallurgy and Materials, Vol. 60, 2015, pp. 149-152

[11]   DEY G.K., MUKHOPADHYAY P. Precipitation in the Ni-Cu-base alloy Monel K-500. Materials Science and Engineering, Vol. 84, 1986, pp. 177-189.

[12]   DEY G.K., TEWARI R., RAO P., WADEKAR S.L., MUKHOPADHYAY P. Precipitation hardening in nickel-copper base alloy Monel K 500. Metallurgical Transactions A, Vol. 24, 1993,pp. 2709-2719.

[13]   ES-SAID O.S., ZAKHARIA K., ZAKHARIA Z., VENTURA C., PFOST D., CRAWFORD P., WARD T., RAIZK D., FOYOS J., MARLOTH R. Failure analysis of K-Monel 500 (Ni-Cu-Al alloy) bolts. Engineering Failure Analysis, Vol. 7, 2000, pp. 323-332.

[14]   AI J.-H., HA H.M., GANGLOFF R.P., SCULLY J.R. Hydrogen diffusion and trapping in a precipitation-hardened nickel-copper-aluminum alloy Monel K-500 (UNS N05500). Acta Materialia, Vol. 61, 2013, pp. 3186-3199.

[15]   SHARP A.G. The coefficient of static friction of Monel K-500 on phosphor bronze. Ocean Engineering, Vol. 4, 1977, pp. 181-186.

[16]   CHEN J., WANG J., YAN F., ZHANG Q., LI Q. Effect of applied potential on the tribocorrosion behaviors of Monel K500 alloy in artificial seawater. Tribology International, Vol. 81, 2015, pp. 1-8.

[17]   CHEN J., YAN F. Tribocorrosion behaviors of Ti-6Al-4V and Monel K500 alloys sliding against 316 stainless steel in artificial seawater. Transactions of Nonferrous Metals Society of China, Vol. 22, 2012, pp. 1356-1365.

[18]   KRAWCZYK J., ADRIAN H. The kinetics of austenite grain growth in steel for wind power plant shafts. Archives of Metallurgy and Materials, Vol. 55, 2010, pp. 91-99.